ELSEVIER

Biochimica et Biophysica Acta 1565 (2002) 196–205

BIOCHIMICA ET BIOPHYSICA ACTA
BBA

www.bba-direct.com

Review

Structural basis for sensory rhodopsin function

Eva Pebay-Peyroula[a], Antoine Royant[a,b], Ehud M. Landau[c], Javier Navarro[c,*]

[a] *Institut de Biologie Structurale, UMR5075, CEA-CNRS-Université Joseph Fourier, 41 rue Jules Horowitz, F-38027 Grenoble Cedex 1, France*
[b] *European Synchrotron Radiation Facility, 6 rue Jules Horowitz, BP 220, F-38043 Grenoble Cedex, France*
[c] *Membrane Protein Laboratory, Department of Physiology and Biophysics, and Sealy Centers for Structural Biology and Molecular Science, The University of Texas Medical Branch, 301 University Boulevard, Galveston, TX 77555-0437, USA*

Received 21 February 2002; received in revised form 2 September 2002; accepted 2 September 2002

Abstract

The crystal structure of sensory rhodopsin II from *Natronobacterium pharaonis* was recently solved at 2.1 Å resolution from lipidic cubic phase-grown crystals. A critical analysis of previous structure–function studies is possible within the framework of the high-resolution structure of this photoreceptor. Based on the structure, a molecular understanding emerges of the efficiency and selectivity of the photoisomerization reaction, of the interaction of the sensory receptor and its cognate transducer protein HtrII, and of the mechanism of spectral tuning in photoreceptors. The architecture of the retinal binding pocket is compact, representing a major determinant for the selective binding of the chromophore, all-*trans* retinal to the apoprotein, opsin. Several chromophore–protein interactions revealed by the structure were not predicted by previous mutagenesis and spectroscopic analyses. The structure suggests likely mechanisms by which photoisomerization triggers the activation of sensory rhodopsin II, and highlights the possibility of a unified mechanism of signaling mediated by sensory receptors, including visual rhodopsins. Future investigations using time-resolved crystallography, structural dynamics, and computational studies will provide the basis to unveil the molecular mechanisms of sensory receptors-mediated transmembrane signaling.

Keywords: Sensory rhodopsin; Signal transduction; Crystallography; Color tuning; Structural mechanism

1. Introduction

Heptahelical transmembrane retinal binding proteins act as energy converters (bacteriorhodopsin and halorhodopsin) or as light sensors (visual and phototaxis rhodopsins). The best studied light sensor, rhodopsin, is a G protein-coupled receptor in the vertebrate retina that uses light to trigger the initial steps in a cascade resulting in vision. In halophilic archaebacteria, sensory rhodopsins (SRI and SRII) are photoreceptors that relay light signals to their cognate transducer proteins (HtrI and HtrII), which in turn initiate a phosphorylation cascade that regulates the cell's flagellar motors in order to control phototaxis. When the bacterium is in need of energy, SRI is activated, mediating migration into illuminated regions, where the proton pump bacteriorhodopsin (bR) is in turn activated and production of ATP takes place. When enough ATP has been synthesized, SRII is activated, mediating repellent phototaxis to darker areas [1]. Alignment of the amino acid sequence of these photoreceptors revealed a high degree of sequence homology in the transmembrane domains, as shown in Fig. 1. The absorption maximum of SRII from *Halobacterium salinarum* is at about 475 nm, and this pigment forms a tightly bound signaling unit with the transducer protein HtrII, which have two transmembrane spanning helices, and conserved cytoplasmic methylation and histidine kinase domains, similar to the homologous bacterial chemotaxis receptor. Currently, the three-dimensional structure of HtrII and related proteins are unknown, as crystallization of membrane proteins is a major hurdle for structural determination. The small amount of SRII in the plasma membrane and its instability in detergents and low ionic strength solutions have precluded comprehensive structure and function studies. On the other hand, the functional homologue of SRII from *Natronobacterium pharaonis* (pSRII) exhibits

Abbreviations: SR, sensory rhodopsin; BR, bacteriorhodopsin; HR, halorhodopsin; TM, transmembrane helices

* Corresponding author. Fax: +1-409-772-1301.
E-mail address: jnavarro@utmb.edu (J. Navarro).

0005-2736/02/$ - see front matter © 2002 Published by Elsevier Science B.V.
PII: S0005-2736(02)00569-2

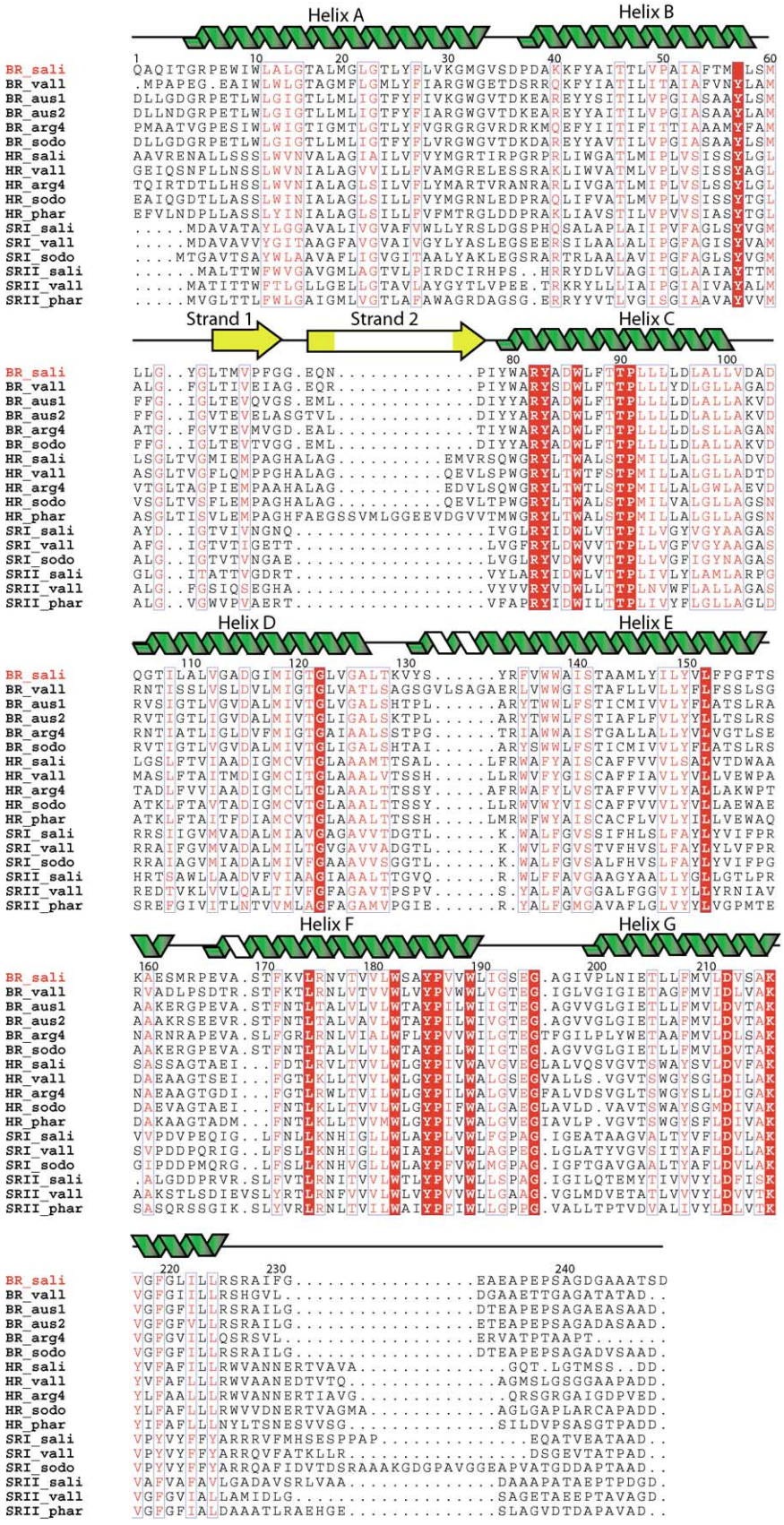
Helix A
Helix B
Strand 1
Strand 2
Helix C
Helix D
Helix E
Helix F
Helix G
BR_sali
BR_vall
BR_aus1
BR_aus2
BR_arg4
BR_sodo
HR_sali
HR_vall
HR_arg4
HR_sodo
HR_phar
SRI_sali
SRI_vall
SRI_sodo
SRII_sali
SRII_vall
SRII_phar

higher stability: it is stable in detergent solutions, and at low ionic strength (down to 50 mM) and high temperatures (range of 0–62 °C). Most importantly, pSRII can be readily overexpressed in *Escherichia coli*. These properties have greatly facilitated the purification of pSRII to homogeneity [2,3], and resulted in it being the best studied sensory rhodopsin. pSRII displays several features: a photophobic response upon illumination, a characteristic absorption spectrum with a maximum peak at 500 nm and shoulder at 470 nm ([4], Fig. 2); and a photocycle with five major spectroscopically defined intermediates (K, L, M, N and O) ([5], Fig. 3). Despite certain similarities with BR, the rate of pSRII ground-state recovery is about two orders of magnitude slower than that of BR, due mainly to the slow decay of the M intermediate. This intermediate is argued to represent the signaling state of pSRII [6], and exhibits a blue-shifted spectrum (λ_{max} = 390 nm), a 13-*cis* retinal configuration and a deprotonated Schiff base. In contrast to BR, large structural changes have been observed upon formation of the K-intermediate in pSRII [7]. Furthermore, and in contradistinction to BR and HR, pSRII does not exhibit light–dark adaptation, as only the all-*trans* retinal is extracted from pSRII in the ground state, which is consistent with the lack of binding of 13-*cis* retinal to the apoprotein opsin [8]. Finally, when not bound to HtrII, pSRII exhibits light-induced proton pumping function as BR, although at very low rates [9]. This proton pumping activity is inhibited when pSRII is bound to the transducer HtrII [10]; however, proton uptake and release still take place in the extracellular surface of pSRII.

SR II is regarded as a paradigm to understand the mechanism of transmembrane signaling, as this photoreceptor shares a number of structural and functional features with visual rhodopsins. Like rhodopsins, pSRIIs display seven transmembrane segments, a conserved Lys residue in helix G that is covalently bound to the chromophore retinal via a protonated Schiff base, and a conserved carboxylic acid counterion to the positively charged Schiff base within helix C (Fig. 4). Furthermore, like rhodopsin, pSRII displays a maximal absorption at around 500 nm; mutagenic disruption of the salt bridge between the Schiff base and the counterion carboxylic residue in helix C causes constitutive activation in the dark [11], and the M photo-intermediate is the signaling state [6]. Finally, photoreceptor activation causes movements of residues in Helix F [12]. Despite these similarities, pSRII has several features distinct from visual rhodopsins. The retinal chromophore is in the all-*trans* configuration in the ground-state of pSRII, whereas in all visual rhodopsins, it is in the 11-*cis* configuration. In addition, rhodopsin couples to the soluble G protein transducin, while pSRII is tightly coupled to integral membrane transducer protein HtrII.

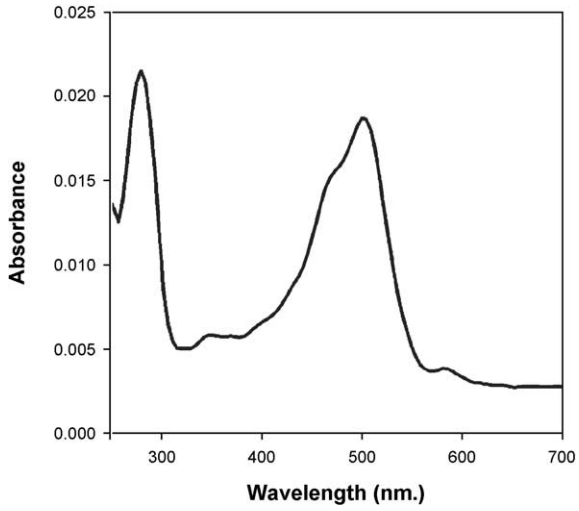

Fig. 2. Ultraviolet–visible absorption spectrum of purified recombinant pSRII in detergent solution. Recombinant pSRII was expressed in *E. coli*, solubilized in β-dodecylmaltoside, and purified by Ni-affinity chromatography as described in Ref. [3]. The spectrum shows the characteristic absorption maximum at 500 nm and a shoulder at 470 nm. This spectrum was recorded in detergent solution and is identical to the spectrum of native pSRII purified from *N. pharaonis* [4].

We have recently delineated the structural basis of the function of pSRII on the basis of its recent X-ray structure to 2.1 Å resolution [13]. Lower resolution structures, from 2D crystals [14], as well as from lipidic cubic phase-grown 3D crystals [15], were recently reported by Spudich's group. In this article, we address three fundamental questions: (a) What insight does the structure provide into the signaling mechanism? (b) What is the structural basis for the mechanism of the "opsin shift" and spectral tuning? (c) What is the mechanism of recognition of HtrII by pSRII?

2. The high-resolution structure of sensory rhodopsin II

2.1. Overview

To obtain well diffracting crystals of pSRII, a C-terminally tagged protein was overexpressed in *E. coli,* purified to homogeneity by Ni-affinity chromatography [3], and crystallized from lipidic cubic phases [16]. Crystals of pSRII in the ground state diffracted to 2.1 Å resolution at the synchrotron [13]. The backbone structure of pSRII is shown in Fig. 5; the protein forms crystallographic dimers, with the A and G helices at the interface, and is arranged in a layered packing. pSRII shows the same absolute absorption spectrum in crystals and in solution, with an absorption maximum at 500 nm and a shoulder at 470 nm (Fig. 6A). Furthermore, upon illumination, pSRII crystals display

Fig. 1. Alignment of the amino acid sequences of halobacterial rhodopsins. Seventeen sequences of BR, HR, SRI, and SRII are analyzed. Species-specific rhodopsins are indicated by four-letter abbreviations following the name of the rhodopsin type. Conserved residues in all rhodopsins are highlighted in red. Residues in boxes are conserved substitutions (pink). Numbering of residues is according to BR from *H. salinarum.* Regions corresponding to the transmembrane helices (A–G, in green), and β-strands (yellow) were assigned according to the crystal structure of BR.

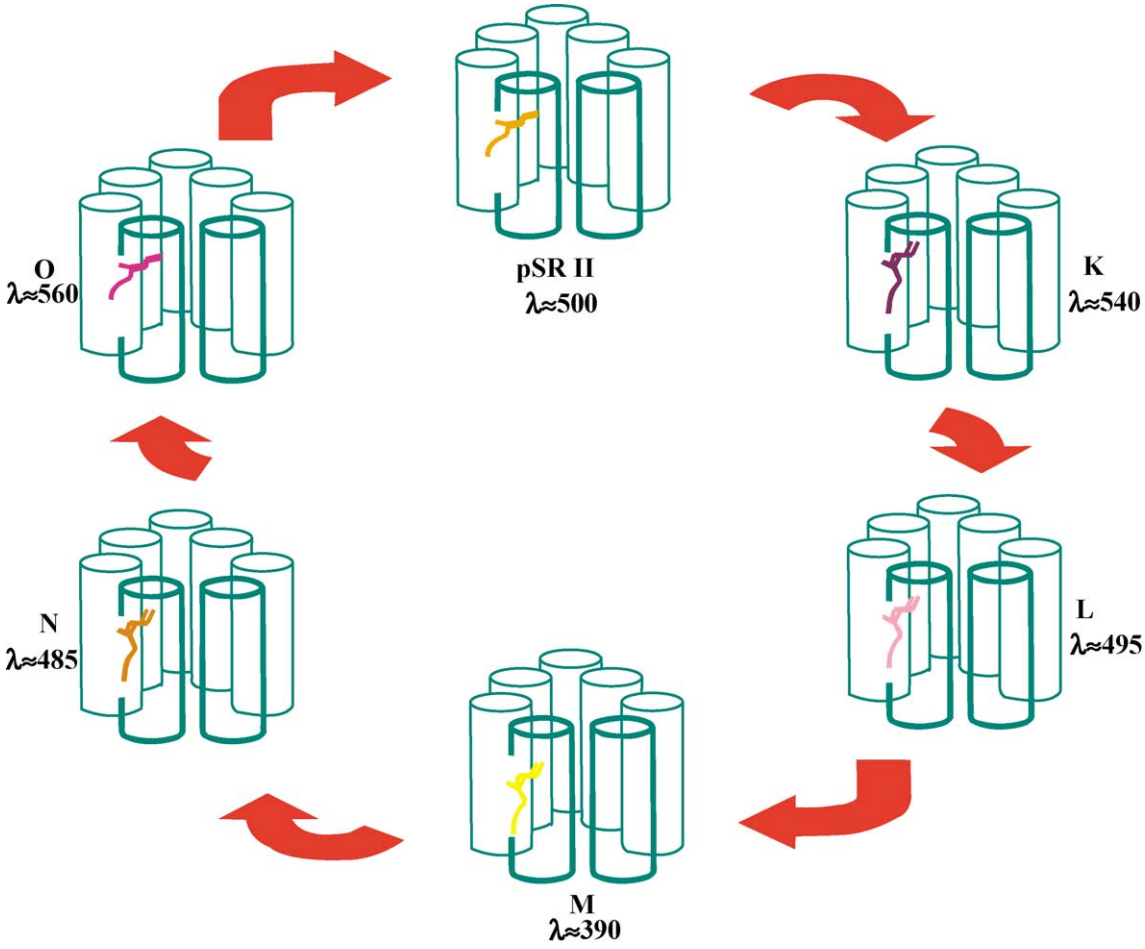

Fig. 3. The photocycle of sensory rhodopsin II from *N. pharaonis*. The retinal chromophore is covalently bound to a Lys-205 in helix G via a protonated Schiff base. The primary reaction, light-induced isomerization of the all-*trans* retinal to 13-*cis* configuration, is followed by thermal reisomerization to the ground state via well-defined spectral intermediates as indicated by the color of the retinal and the λ_{max} of the intermediates.

characteristic photo-intermediates, suggesting that the photoreceptor is functional in crystals. The spectrum of the K-intermediate at low temperatures is shown in Fig. 6B,C.

Despite their different functions, the structures of the seven transmembrane helices in SRII, BR and HR are highly conserved, as shown by superposition of the structure of pSRII on those of BR and HR [13]. Helices C–G shows the highest similarity, with r.m.s. deviations (r.m.s.d.) on the main chain atoms of 0.77 Å (pSRII-BR) and 0.89 Å (pSRII-HR), respectively, consistent with the idea that the pentahelical C–G fragment represents a conserved core of archaeal rhodopsins [17]. Like BR and HR, the extracellular surface of pSRII consists of an amino terminal and three interhelical loops with significant secondary structure. Thus, these three photoreceptors exhibit a conserved BC loop organized as an antiparallel β-sheet.

2.2. Active site of pSRII

A view of the molecular architecture of the active site of pSRII reveals that the Schiff base of the retinal separates the hydrophobic cytoplasmic half of pSRII from the hydrophilic extracellular half. Fig. 7 shows the backbone in ribbon representation, and the residues within 5 Å of the retinal chromophore. Substitutions of these residues give rise to red shifts in the absorption maximum of pSRII [18,19]. The high resolution X-ray structure shows the retinal in the all-*trans* configuration, with the β-ionone ring in the 6-s-*trans* configuration. The position and orientation of the residues that comprise the retinal-binding pocket constrain the chromophore into an almost planar conformation, in contrast to the twisted conformation in solution. Like HR and BR, the G helix is distorted by adopting a π bulge conformation around Lys-205. Of great significance is the guanidinium group of Arg-72, which points toward the extracellular side of the membrane in pSRII, unlike the orientation of the corresponding Arg-82 in BR; this results in a larger distance to Asp-75. This larger distance may contribute to the elevated pK_a of 5.6 of Asp-75, compared to the pK_a of 2.2 for the corresponding Asp-85 in BR [5]. $2F_{obs} - F_{calc}$ and $F_{obs} - F_{calc}$ maps reveal an unusually high electron density near the extracellular side of helix C. We suggest that this density corresponds to a chloride ion, which is in accord with reports of chloride-induced spectral shifts of

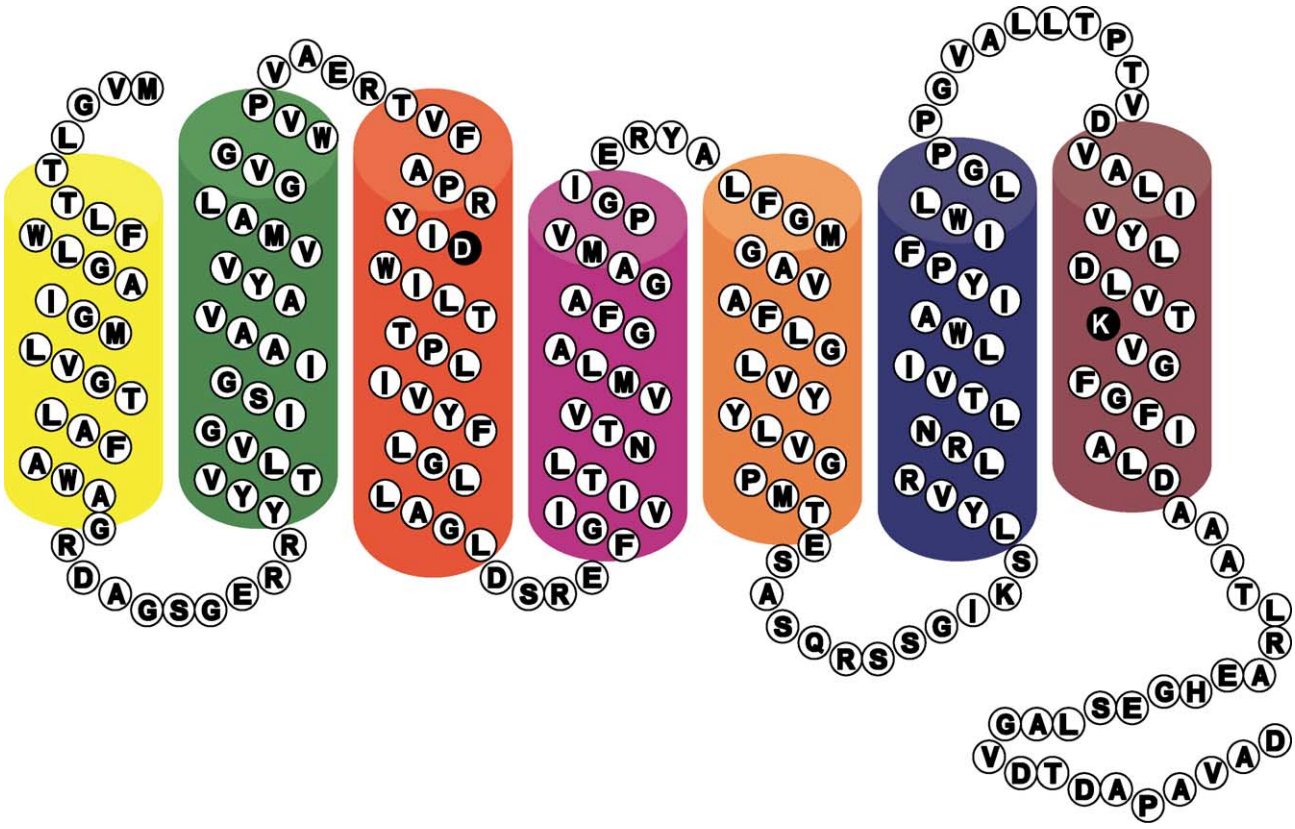

Fig. 4. Two-dimensional model of sensory rhodopsin II from *N. pharaonis*. Amino acid residues are depicted in single-letter code. The N-terminus, as well as the extracellular domains, are at the top, and the C-terminus and intracellular domain are at the bottom. Transmembrane α-helices are shown as colored cylinders. The counterion Asp-75 in helix C, and the Lys-205 in helix G are shown in black circles.

pSRII [20]. Most importantly, at 2.1 Å resolution, we have identified water molecules in the extracellular channel, which are assembled in a complex H-bonding network with polar residues and the chloride ion in the active site (Fig. 8). The most prominent features of this network are that the protonated Schiff base is linked to Asp-75 and Asp-201 via H-bonds to Wat-402. In addition, the putative chloride ion is coupled to the Schiff base by a H-bonding network, involving coordination to Arg-72, Tyr-73, Wat-406 and Wat-407, and the N–H of the backbone amide of Phe69. Interestingly, Wat-405 bridges Arg-72 to Asp-193 in the extracellular channel via H-bonding. It is feasible that this linkage and the presence of a chloride ion regulate the pK_a of Asp-193. The architecture of the H-bonding network in the extracellular channel of pSRII is therefore distinct from that of BR, and consistent with recent FTIR studies, indicating that hydrogen bonds are weaker in pSRII than in BR [21].

3. The mechanism of transmembrane signaling

The molecular basis underlying the transmembrane signaling mediated by sensory receptors is still unclear, as the ground state structure of pSRII represents only a single snapshot in the trail of events leading to the formation of the signaling state (M intermediate). However, the proximity and orientation of the functional groups and water molecules in the ground state structure should allow a rational hypothesis of the molecular mechanism by which photoisomerization of the retinal triggers the generation of the signaling state. Particularly, the ground-state structure of pSRII should help in formulating the structural basis for the selectivity and efficiency of the transmembrane signaling mediated by pSRII. In the first instance, the ground-state structure reveals that the all-*trans* retinal, but not other isomers, fits well into the retinal pocket, indicating that the architecture of the binding site is the key determinant for conferring specificity to ligand binding (Fig. 9). This finding agrees with previous experiments indicating that pSRII binds selectively all-*trans* retinal [8]. The unique environment provided by the architecture of the retinal-binding pocket is the structural basis determining the selectivity and efficiency of the photoisomerization. The polyene chain of the retinal is highly constrained by the hydrophobic residues Trp-76, Trp-171 and Tyr-174. A hydrophobic cavity (defined mainly by Trp-178, Phe-127, and Val-108) loosely accommodates the β-ionone ring, in good agreement with previous studies indicating that opsin of pSRII binds ring-modified retinals [22]. On the other hand, the protonated Schiff base is localized within a polar environment delineated by the counterion Asp-75, Asp-201 and water molecules assembled as a H-bonding network on the extrac-

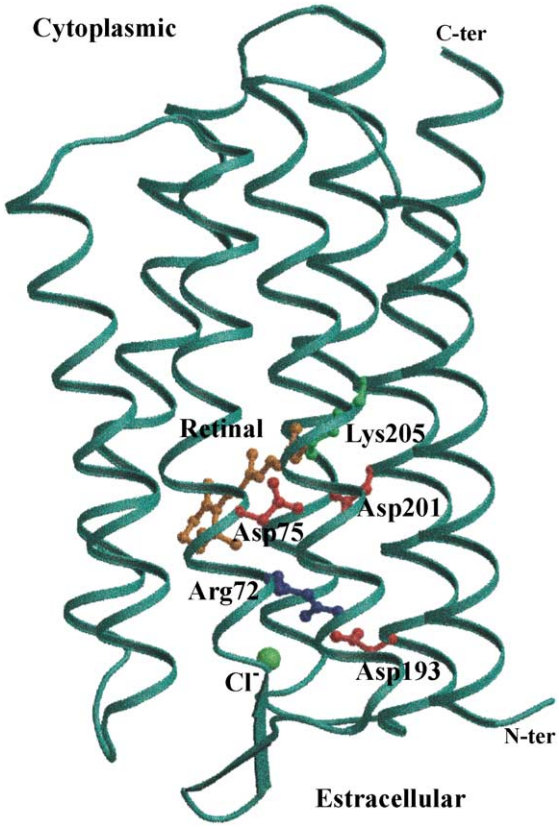

Fig. 5. Cα trace representation of sensory rhodopsin II. Diagram was derived from the 2.1 Å crystal structure coordinates. The N-terminus and the extracellular domain are at the bottom, while the C-terminus and intracellular domain is toward the top. The retinal chromophore is shown in orange. Key residues in the binding pocket are highlighted. The structure was derived from the coordinates of the 2.1 Å resolution structure (PDB ID code 1h68).

ellular side of the receptor. In this environment, the all-*trans* retinal, bound as a protonated Schiff base, photoisomerizes selectively to the 13-*cis* configuration with high efficiency within 5 ps after illumination. This reaction is in stark contrast to the photoisomerization of the protonated Schiff base of all-*trans* retinal in solution, which is neither selective nor efficient; in solution, the chromophore isomerizes upon illumination to form a mixture of the 9-*cis*, 11-*cis* and 13-*cis* isomers, with efficiencies of 2%, 14%, and 1% respectively [23]. Of particular importance, the structure reveals that the molecular assembly of the salt bridge between the protonated Schiff base and its counterion is mediated by the water molecule Wat-402. Disruption of this salt bridge is a key event in the formation of the signaling M intermediate; however, the molecular mechanism for the generation of this signaling state as well as the steps leading to the regeneration of the ground state remain to be elucidated. Although the ground-state structure of pSRII represents a single state in the signal transduction pathway, we envision that light-induced isomerization of the all-*trans* retinal would give rise to a conformationally strained 13-*cis* retinal, as the retinal binding pocket can only accommodate all-*trans* retinal. Relaxation of the 13-*cis* retinal should involve structural rearrangements in the active site. We suggest that upon photoisomerization, the protonated Schiff base reorients, weakening its interaction with Wat-402. In turn, the H-bonding network is disrupted, weakening the interaction of Asp-75 with Arg-72, which is involved in controlling the pK_a of Asp-75. These structural changes should increase the pK_a of Asp-75, and decrease the pK_a of the Schiff base. The changes in pK_a should in turn facilitate the proton transfer from the Schiff base to Asp-75, disrupting this linkage and generating the blue-shifted signaling M intermediate. In this new configuration of the retinal binding

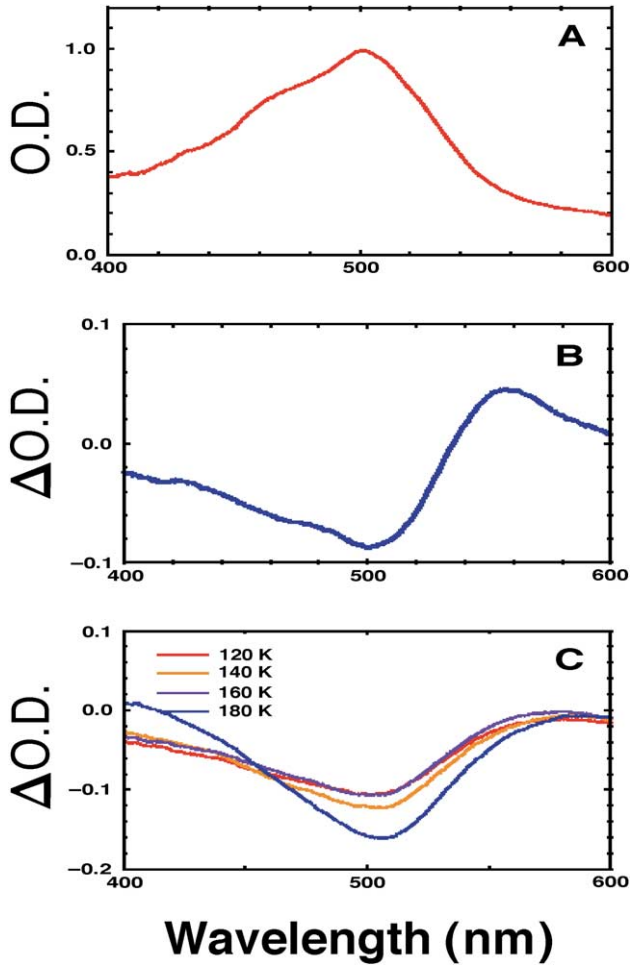

Fig. 6. Absolute and difference absorption spectra of single sensory rhodopsin II crystals grown from lipidic cubic phases. (A) The absolute absorption spectrum of sensory rhodopsin II crystals recorded with a microspectrophotometer as previously described [34]. (B) Difference spectra were obtained by subtracting the spectrum of an illuminated crystals with green light ($\lambda = 532$ nm) at 170 K from the spectrum of unilluminated crystals at the same temperature. (C) Same as in (B) except that spectra were recorded at various temperatures. The red-shifted peak in the difference spectra indicates the formation of the K-intermediate, whereas the negative peaks indicate the depletion of the ground-state sensory rhodopsin II.

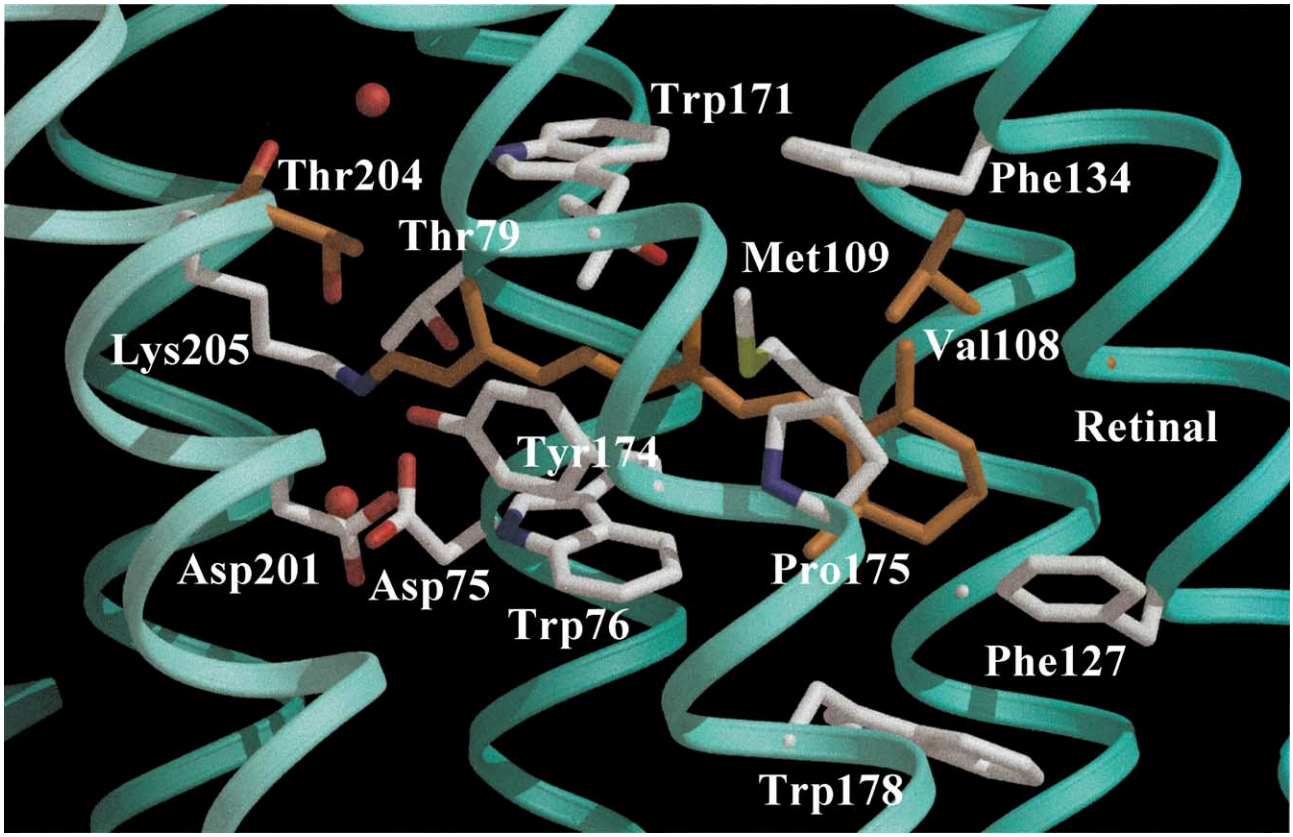

Fig. 7. The chromophore binding pocket of sensory rhodopsin II. The retinal is shown in orange and key residues within 5 Å are indicated in green. Residues Val-108 and Thr-204 are involved in color tuning and are conserved in sensory rhodopsin II from different species.

pocket, the chromophore may thermally relax by initiating an upward movement of the 9- and 13-methyl groups of the retinal, pushing Trp-171 in helix F toward the cytoplasmic side, thereby disrupting the hydrogen bonding between Trp-171 and Thr-204 in helix G, thus contributing to the tilting of helix F, reorientation of helix G, and switching of the Schiff base toward the cytoplasmic side. The movements of the F and G helices are in agreement with previous spin-labeling experiments, indicating that the formation of the signaling intermediate involves tilting of helix F and reorientation of helix G [12]. Similar structural changes have been detected in the mechanism of signaling mediated by visual rhodopsin, as well as in the mechanism of proton transport by BR, highlighting the concept of a unified mechanism of action of retinal photoreceptors and perhaps of G protein-coupled receptors [24,25]. In this respect, a key question is: what is the functional significance of the global structural changes of the F and G helices? One possibility is that the transmission of the light signal to the HtrII transducer is mediated by displacement of helices F and G, which functionally interact with the second transmembrane helix (TM2) in HtrII via helix–helix interaction. A second possibility is that the displacement of the F and G helices is not involved in the transmission of the signal, but instead opens up the cytoplasmic channel for reprotonation of the Schiff base. The latter possibility is supported by the observation that the mutant D73N mutant of SRII from *H. salinarum*, in which the salt bridge is disrupted, is constitutively active [11]. Furthermore, in contrast to wild-type pSRII, the D75N mutant does not form the M intermediate upon illumination, and the cytoplasmic channel is closed, as demonstrated by the resistance of this mutant to bleaching by the water-soluble reagent hydroxylamine [26]. Based thereon, we argue that disruption of the salt bridge is the major trigger for receptor activation, and that short-range structural changes in the helices might mediate the signal transmission to HtrII via helix–helix interaction.

4. Signal transmission to HtrII

A critical question in phototransduction is: how does the receptor transmit the light signal to the transducer protein? Previous experiments have suggested that the specificity of the sensory rhodopsin/transducer interaction is determined by the nature of the two transmembrane helices and a stretch of 90 residues following the cytoplasmic end of TM2 of the transducer, and the nature of F and G helices of the sensory receptor [27,12]. PSRII and HtrII appears to be bound with a stoichiometry of 2:2 [28]. However, the identity of the

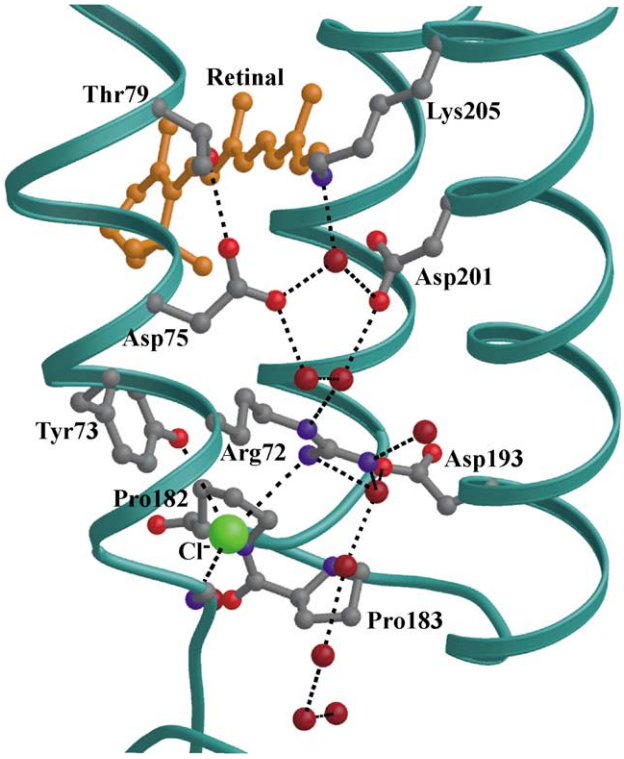

Fig. 8. Hydrogen-bonding network between the retinal binding site and the extracellular surface. The retinal is colored in orange, the water molecules are shown in dark red, while the chloride ion near the extracellular surface is depicted as a green sphere. Hydrogen bonds are shown as dotted lines. In contrast to BR, the side chain of Arg-72 is oriented toward the extracellular side of the membrane.

interacting residues, and the nature of their interactions at the interface of the sensory receptor/transducer complex, are unknown. The surface of pSRII reveals a unique patch of charged and polar residues at the cytoplasmic ends of helices F (Lys-157, Ser-158, Arg-162, Arg-164, and Asn-165) and G (Asp-214) (Fig. 10). This patch is not present in BR or HR [13]. It is thus likely that these positively charged residues interact electrostatically with the negatively charged cytoplasmic domain Gly-Asp-Gly-Asp-Leu-Asp of transmembrane helix 2 of HtrII, which is conserved among various species [29]. The extraordinary stability of the pSRII–HtrII complex [12] may be explained by this electrostatic interaction, which it is further enhanced by the low-dielectric environment of the lipid bilayer. Interestingly, Ser-158 and Phe-210, located in the cytoplasmic side of helices F and G, respectively, point outwards (Fig. 10). We propose that transmission of the light signal from the receptor to HtrII is mediated by means of the interaction of Ser-158 and Phe-210 with TM2 of HtrII. This model is in agreement with recent results from EPR experiments [12], indicating that light-induced mobility of spin-labeled Ser-158 is restrained in the presence of HtrII, and also in agreement with the recent observation that HtrII closes the cytoplasmic channel of pSRII [30].

5. The mechanism of spectral tuning in archeabacterial rhodopsins

The free protonated Schiff base form of retinal in solution absorbs at about 440 nm, whereas the same chromophore bound to the apoprotein displays a red spectral shift, an effect known as the ‘‘opsin shift’’. Visual receptors provide an example for spectral tuning; the cone cells of the human retina contain pigments absorbing in the blue (425 nm), green (530 nm), and red (560 nm) regions of the spectrum, providing the physical basis for the sense of color. However, the mechanisms by which the apoprotein opsin regulates the λ_{max} of the chromophore is not clear yet.

The absorption maximum of 500 nm of pSRII is significantly blue-shifted with respect to those of BR, HR, and SRI (λ_{max} of 560–590 nm). However, replacement of 10 residues in pSRII by the corresponding residues of the active site of BR resulted only in a 24 nm red shift [19], suggesting that the molecular architecture of the pSRII retinal pocket is different from that of BR and plays a key role in spectral tuning. To further understand the underlying mechanisms of spectral tuning, the photoreceptor spectral shifts were recently computed on the basis of the high resolution structures the two homologous retinal proteins, BR and pSRII, with spectral maxima of 570 and 500 nm, respectively [35]. Superposition of these two structures revealed a displacement of the G helix of pSRII toward the cytoplasmic side, which could explain the absence of dark adaptation (partial formation of the 13-*cis*,15-*syn* retinal isomer) in pSRII [8]. The displacement of this helix, to which the retinal is covalently bound (via a protonated Schiff base linkage to Lys-205), decreases the flexibility of retinal needed to adopt the bent conformation of the 13-*cis*, 15-*syn* isomer. Such a correlation between chromophore isomerization and the movement of helix G is also evident from the recent X-ray structures of BR intermediates [31]. The results of these quantum mechanical calculations successfully explain the difference between the spectra in BR and pSRII [35]. The analysis of the calculated energies shows that the observed difference is mainly due to electronic reorganization in retinal. In comparison to BR, a shift in the relative position of helix G, and consequently a shorter distance between the counterion and the Schiff base group of the chromophore in pSRII seems to be the main reason for the observed blue shift of the spectrum. This concept is consistent with previous data indicating that the hydrogen bond between the Schiff base and its counter-ion in pSRII is stronger than that in BR [32]. The calculated energy levels for the excited states of retinal also provide an explanation for the observed shoulder in the spectrum of pSRII, attributing this feature to the S_2 state of retinal in pSRII. The successful explanation of the BR-to-pSRII spectral shift opens the door to investigations that seek to explain the molecular mechanism for spectral tuning in visual pigments on the basis of ab initio quantum chemical calculations. In contrast, recent calculations by [33] con-

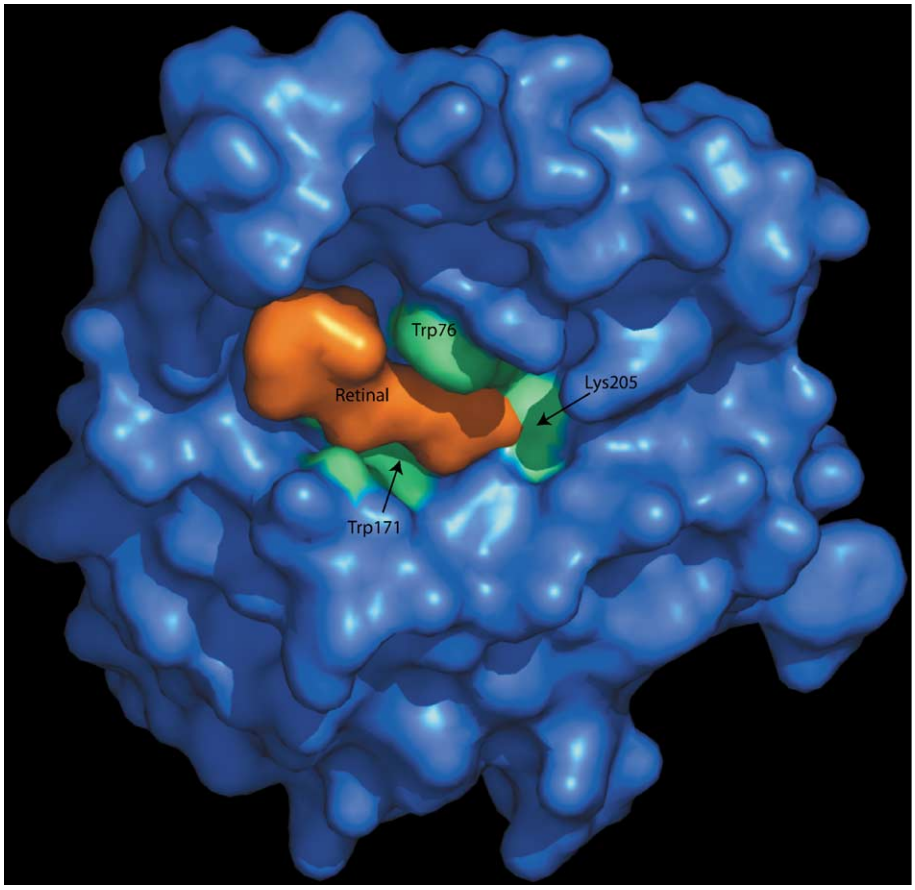

Fig. 9. The retinal binding site of sensory rhodopsin II. A cut-away surface is depicted from the extracellular side. Residues on the top of the retinal are detached to visualize the retinal pocket. The opsin is colored blue, the retinal is shown in orange and the indicated residues are colored in green. This figure was produced using the program PyMol [36].

cluded that the main source of the blue shift of pSRII is associated with the different orientations of Arg-72 (Arg-82 in BR) in the two proteins. However, substitution of Arg-72 to Ala did not shift the maximum absorption (unpublished observations), suggesting that Arg-72 does not play a major role in the spectral shift of pSRII.

6. Concluding remarks

The high-resolution structure of pSRII has revealed the positions of water molecules within the active site of the protein. These molecules are essential for the formation of the H-bonding network that confers stability and functionality to the receptor. The application of spectroscopic methods in the context of the high-resolution structure should permit a comprehensive analysis of the structure/function relationship. Analysis of the architecture of the retinal-binding pocket established the structural basis of the ligand selectivity, consistent with the specific binding of the all-*trans* retinal with the opsin. Furthermore, the structure reveals the pathway for proton transfer from the Schiff base to Asp-75, an event which is important for the generation of the signaling M intermediate. Based on the high-resolution structure, we can now propose a possible mechanism for the selectivity and efficiency of transmembrane signaling mediated by pSRII. We have identified a positively charged patch at the cytoplasmic end of helices F and G, which might interact with a negatively charged sequence in the cytoplasmic domain of the transducer HtrII. Finally, comparison of the highly similar structures of BR and pSRII have provided the basis to apply computational methods to elucidate the physical mechanism for the spectral shifts exhibited by these photoreceptors. Future studies will include co-crystallization and structural elucidation of the pSRII–HtrII complex, and structural dynamic experiments to unveil the exact nature of the conformational changes associated with function.

Acknowledgements

We are grateful to Carrie A. Maxwell for expert technical help, to members of the Membrane Protein Laboratory for comments, and Karl Edman, S. Hayashi, Richard Neutze, Peter Nollert, K. Schulten, Bryan Sutton, E. Tajkhorshid, and Marisa E. Vasquez for their experimental contributions,

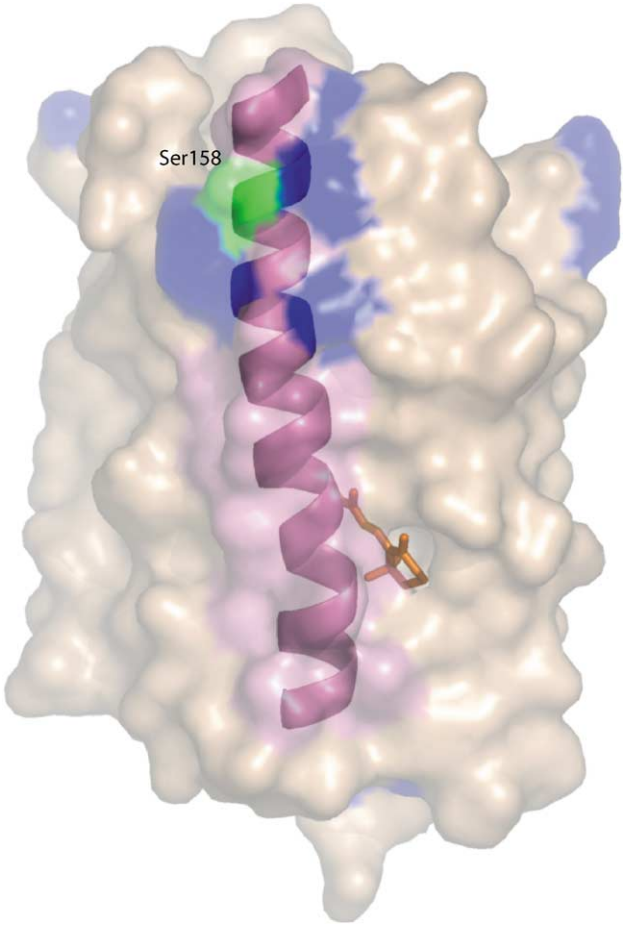

Fig. 10. Surface representation of sensory rhodopsin II. A positively charged patch on the cytoplasmic surface of helix F of sensory rhodopsin II is colored in blue. This patch is a putative binding site for the transducer HtrII. Ser-158 is shown in green and is suggested to play a role in transmitting the light signal from the retinal binding pocket to HtrII. This figure was produced using the program PyMol [36].

insightful discussions and art work. Support was provided by grants from Howard Hughes Medical Institute, the Welch Foundation, American Heart Association, NIH RO1 GM64855, Swiss National Science Foundation, the French Ministry of Education and Research, and the European Union-BIOTECH.

References

[1] J.L. Spudich, C.S. Yang, K.H. Jung, E.N. Spudich, Annu. Rev. Cell Dev. Biol. 16 (2000) 365–392.
[2] K. Shimono, M. Iwamoto, M. Sumi, N. Kamo, FEBS Lett. 420 (1997) 54–56.
[3] I.P. Hohenfeld, A.A. Wegener, M. Engelhard, FEBS Lett. 442 (1999) 198–202.
[4] J. Hirayama, Y. Imamoto, Y. Shichida, N. Kamo, H. Tomioka, T. Yoshizawa, Biochemistry 31 (1992) 2093–2098.
[5] I. Chizhov, G. Schmies, R. Seidel, J.R. Sydor, B. Luttenberg, M. Engelhard, Biophys. J. 75 (1998) 999–1009.
[6] B. Yan, T. Takahashi, R. Johnson, J.L. Spudich, Biochemistry 30 (1991) 10686–10692.
[7] A. Losi, A.A. Wegener, M. Engelhard, W. Gartner, S.E. Braslavsky, Biophys. J. 78 (2000) 2581–2589.
[8] J. Hirayma, N. Kamo, Y. Imamoto, Y. Shichida, T. Yoshizawa, FEBS Lett. 364 (1995) 168–170.
[9] G. Schmies, B. Luttenberg, I. Chizhov, M. Engelhard, A. Becker, E. Bamberg, Biophys. J. 78 (2000) 967–976.
[10] Y. Sudo, M. Iwamoto, K. Shimono, M. Sumi, N. Kamo, Biophys. J. 80 (2001) 916–922.
[11] E.N. Spudich, W. Zhang, M. Alam, J.L. Spudich, Proc. Natl. Acad. Sci. U. S. A. 94 (1997) 4960–4965.
[12] A.A. Wegener, I. Chizhov, M. Engelhard, H.J. Steinhoff, J. Mol. Biol. 301 (2000) 881–891.
[13] A. Royant, P. Nollert, K. Edman, R. Neutze, E.M. Landau, E. Pebay-Peyroula, J. Navarro, Proc. Natl. Acad. Sci. U. S. A. 98 (2001) 10131–10136.
[14] E.R. Kunji, E.N. Spudich, R. Grisshammer, R. Henderson, J.L. Spudich, J. Mol. Biol. 308 (2001) 279–293.
[15] H. Luecke, B. Schobert, J.K. Lanyi, E.N. Spudich, J.L. Spudich, Science 293 (2001) 1499–1503.
[16] E.M. Landau, J.P. Rosenbusch, Proc. Natl. Acad. Sci. U. S. A. 93 (1996) 14532–14535.
[17] M. Kolbe, H. Besir, L.O. Essen, D. Oesterhelt, Science 288 (2000) 1390–1396.
[18] K. Shimono, M. Iwamoto, M. Sumi, N. Kamo, Photochem. Photobiol. 72 (2000) 141–145.
[19] K. Shimono, Y. Ikeura, Y. Sudo, M. Iwamoto, N. Kamo, Biochim. Biophys. Acta 1515 (2001) 92–100.
[20] J. Sasaki, J.L. Spudich, Biochim. Biophys. Acta 1460 (2000) 230–239.
[21] H. Kandori, Y. Furutani, K. Shimono, Y. Shichida, N. Kamo, Biochemistry 40 (2001) 15693–15698.
[22] J. Hirayama, Y. Imamoto, Y. Shichida, T. Yoshizawa, A.E. Asato, R.S. Liu, N. Kamo, Photochem. Photobiol. 60 (1994) 388–393.
[23] Y. Koyama, K. Kubo, M. Komori, H. Yasuda, Y. Mukai, Photochem. Photobiol. 54 (1991) 433–443.
[24] H.J. Steinhoff, R. Mollaaghababa, C. Altenbach, K. Hideg, M. Krebs, H.G. Khorana, W.L. Hubbell, Science 266 (1994) 105–107.
[25] D.L. Farrens, C. Altenbach, K. Yang, W.L. Hubbell, H.G. Khorana, Science 274 (1996) 768–770.
[26] M. Iwamoto, Y. Sudo, K. Shimono, N. Kamo, Biochim. Biophys. Acta 1514 (2001) 152–158.
[27] X.N. Zhang, J. Zhu, J.L. Spudich, Proc. Natl. Acad. Sci. U. S. A. 96 (1999) 857–862.
[28] A.A. Wegener, J.P. Klare, M. Engelhard, H.J. Steinhoff, EMBO J. 20 (2001) 5312–5319.
[29] R. Seidel, B. Scharf, M. Gautel, K. Kleine, D. Oesterhelt, M. Engelhard, Proc. Natl. Acad. Sci. U. S. A. 92 (1995) 3036–3040.
[30] Y. Sudo, M. Iwamoto, K. Shimono, N. Kamo, Biochim. Biophys. Acta 1558 (2002) 63–69.
[31] H. Luecke, Biochim. Biophys. Acta 1460 (2000) 133–156.
[32] H. Kandori, K. Shimono, Y. Sudo, M. Iwamoto, Y. Shichida, N. Kamo, Biochemistry 40 (2001) 9238–9246.
[33] L. Ren, C.H. Martin, K.J. Wise, N.B. Gillespie, H. Luecke, J.K. Lanyi, J.L. Spudich, R.R. Birge, Biochemistry 40 (2001) 13906–13914.
[34] K. Edman, P. Nollert, A. Royant, H. Belrhali, E. Pebay-Peyroula, J. Hajdu, R. Neutze, E.M. Landau, Nature 401 (1999) 822–826.
[35] S. Hayashi, E. Tajkhorshid, E. Pebay-Peyrula, A. Royant, E.M. Landau, J. Navarro, K. Shulten, J. Phys. Chem. 105 (2001) 10124–10131.
[36] W.L. DeLano, The PyMOL Molecular Graphics System, DeLano Scientific, San Carlos, CA, USA, 2002. http://www.pymol.org.